Clinical trial

Clin Ter 2020; 171 (5):e385-392. doi: 10.7417/CT.2020.2245

Effect of a laser-ablated micron-scale modification of dental implant collar surface on changes in the vertical and fractal dimensions of peri-implant trabecular bone

R. Guarnieri[1], G. Miccoli[1], D. Di Nardo[1], M. D'Angelo[1], A. Morese[1], M. Seracchiani[1], L. Testarelli[1]

[1]*Department of Oral and Maxillo-Facial Sciences, Sapienza University of Rome, Italy*

Abstract

Background. Marginal bone loss (MBL) represents an important indicator of peri-implant health and the measure of its level is considered a determining factor in the evaluation of the quality of survival. Aim of this study is to compare radiographic changes in the fractal and mesial/distal vertical dimensions of peri-implant trabecular bone of dental implants with a laser-ablated micron-scale modication (LAM) of collar surface after a 5-year follow-up period.

Materials and methods. Thirty-four implants with LAM of collar surface (test group = TG) and 31 implants without LAM of collar surface (control group = CG) were placed in 45 non-smoking, periodontally healthy patients. Fractal and vertical dimensions of peri-implant trabecular bone were measured by comparing radiographs taken immediately after prosthesis delivery with those taken 3 years and 5 years after functional loading.

Results. At the end of the 5-year follow-up, the MBL in the TG was 0.87±0.21 and 0.75±0.25 mm at the mesial and distal aspects, respectively, while a MBL of 2.05±0.25 mm at the mesial aspect and 2.01±0.34 mm at the distal site was recorded in the CG. A statistically significant difference was noted. In the TG the mean fractal dimension before loading was 1.4213±0.0525. It increased significantly to 1.4329±0.0479 at 3 years after loading and remained almost stable at 5 years after loading (1.4327±0.0291). In the CG the mean fractal dimension before loading was 1.4119±0.0414. It increased significantly to 1.4282±0.0324 at 3 years after loading and decreased significantly to 1.4111±0.0624 at 5 years after loading. At the end of the follow-up, differences between both study groups were statistically significant.

Conclusions. The increased fractal dimension and the reduced MBL around TG implants after 5 years of functional loading indicates a positive effect of a laser-ablated micron-scale modication of collar surface on peri-implant trabecular bone remodeling. ***Clin Ter 2020; 171 (5):e385-392. doi: 10.7417/CT.2020.2245***

Key words: *Peri-implant bone remodeling, Dental implants, Laser-microgrooved collar, Fractals*

Introduction

In last years one of the most important focuses in implant dentistry has been the study of marginal bone loss (MBL) patterns to better achieve a predictable and long-term esthetic and healthy result (1,2). The concept of MBL after prosthetic reconstruction of an dental implant was introduced by Albrektsson et al. (3) more than two decades ago. MBL represents an important indicator of peri-implant health, and the measure of its level is considered a determining factor in the evaluation of the quality of survival as peri-implant bone loss may induce pocket formation (4,5). The values generally accepted as a reasonable guideline for MBL are 1.5 mm for the first year following loading of the implants and 0.2 mm of additional loss for each subsequent year (3,4). Several studies have reported that MBL may result from implant design, density of bone, surgical trauma at implant insertion, occlusal overload, apical migration of the crevicular epithelium in an attempt to isolate bacterial-induced infection or to establish a biological width, blood supply interruption, or development of a pathogenic bacterial biofilm, periodontal status, and smoking habit (6). However, the precise mechanisms of this phenomenon are not yet completely known. The influence of the implant collar surface on MBL around implants has been discussed only recently and has received little attention in comparison with other factors (7). Dental implant collars have traditionally smooth surfaces to prevent the accumulation of plaque along the top edge of the implant, but this too is considered a contributor to marginal bone die-back to the first implant thread (3). The process of peri-implant soft tissue/implant integration has been characterized at the histologic level (8). Architecturally, a connective tissue attachment and junctional epithelial attachment are reproducibly formed along the implant collar. However, the implant collar/peri-implant mucosa interface is readily distinguished from the tooth-tissue interface in several ways. A direct attachment of connective tissue into cementum as Sharpey's fibers has not been observed. At implant collar, a dense collagenous connective tissue is oriented with the collagen fibers circumferential to the collar surface. Importantly, the organization

Correspondence: Dario Di Nardo, Department of Oral and Maxillo Facial Sciences Sapienza University of Rome. Via Caserta, 6 – 00161 Rome, Italy. Email: dario.dinardo@uniroma1.it Phone: +39 3393935527

ISSN 1972-6007

of this tissue is not related to the superimposed architecture of the prosthesis or the abutment, and this creates significant challenges in esthetic implant dental therapy. In recent years, some strategies have been developed to improve peri-implant tissue integration. One of these strategies is using a laser-ablated micron-scale modication (LAM) of collar surface (Figure 1). Tissue culture studies (9-12) evaluating the effect LAM of implant collar surface with regard to attachment, spreading, orientation, and growth of fibroblasts, showed that cultured fibroblasts grown on 8 micron laser microgrooved surfaces become oriented and channeled in line with the grooves, whereas cells grown on nongrooved surfaces showed random growth. Furthermore, laser-ablated 8 micron grooves promote oriented cell filipodial contact and fibrin fibril orientation. These in vitro results have provided the hypothesis that 8 micron LAM surfaces could be used to control soft tissue responses to implant surfaces. It has in fact been suggested that on dental collar implants, the LAM surface might act to establish a predetermined site to attract a physical connective tissue attachment. Histologic research in an animal model and in humans has subsequently confirmed this hypothesis, documenting the presence of a physical connective tissue attachment onto laser-produced microgrooves on implant collar surfaces (13-16). The most important aspects of this physical connective tissue attachment may be the fact that its position is determined by the layout of the laser microgrooves, with the connective tissue fibers perpendicularly oriented to the implant surface; these fibers act as a seal to apical migration of gingival epithelial cells and fibroblasts. However, the biological and clinical impact of this novel kind of attachment must continue to be investigated, especially in terms of stability over time and hard/soft tissue level maintenance (17-20). Periapical radiographs, which are frequently taken during routine dental examination, are traditionally interpreted by measuring peri-implant MBL. Unfortunately, this most commonly used method has low sensitivity (21) and has been shown to be of limited diagnostic value for the detection of changes in bone (22). As a result, there has been a search for available, reliable, and sensitive methods of assessment, offering affordable and more accessible ways to measure peri-implant trabecular changes. Recent studies have suggested that fractal dimension analysis is a noninvasive tool that can be used to describe biological systems in clinical studies and is a method of identifying scale-invariant structure that is not affected by exposure or minor alignment variations on radiographs (23,24). It is thus well suited to the analysis of three-dimensional trabecular bone patterns on plain radiographs. Several studies have found a strong correlation between the demineralization of alveolar bone and decreasing fractal dimension (25-27). The aim of this study was to compare radiographic changes in the fractal and mesial and distal vertical dimensions of peri-implant trabecular bone of dental implants with a laser-ablated micron-scale modication (LAM) of collar surface, to implants without LAM after a 5-year follow-up period.

Material and methods: This study was designed as a retrospective clinical and radiographic analysis. Implants were divided into two groups:

1) The test group (TG): implants with LAM collar surface; the most coronal 1.8 mm being laser-microtextured (BioHorizons Laser-Lok"; Internal Implants, Birmingham, AL, USA);
2) The control group (CG): implants without LAM collar surface; the most coronal 0.3 mm being smooth, machined metal and the next 1.5 mm of the collar treated with resorbable blast texturing (BioHorizons RBT; Internal Implants, Birmingham, AL, USA).

Both implants have the same tapered macro design, with the same body RBT surface, and the same buttress threads. The TG implant has a laser-ablated micron-scale modication that imparts circumferential, isotropic channels onto the titanium surface (Fig. 1).

This research study used a retrospective clinical database that included patients who were previously treated either as part of an approved research protocol or as part of routine periodontal care using accepted therapy for each patient's specific clinical needs. As the current research involves a retrospective analysis of pre-existing data and current investigators did not have access to identifi- able private information, this research did not require approval by an institutional ethics board or committee. Written informed consent was obtained, and the study was conducted according to the principles of the Declaration of Helsinki on experimentation involving human subjects. The subjects were recruited from the patient pool of two private italian dental clinics. The clinical charts of patients receiving a dental implant with either a LAM collar surface or without a LAM collar surface were screened. No randomization was performed, being this a retrospective study, and the choice of the implant type depended on the clinician and on the stock availability.

Out of this cohort, 45 patients, who had received a total of 65 dental implants, were available for re-evaluation after 5 years.

To be included in the study, the following criteria had to be fulfilled: age ≥18 years, implants placed in native bone; availability of a periodontal chart and periapical radiograph obtained using the parallel long cone technique at the time of crown insertion and at the 3- and 5- year follow-up period; implants supported a single crown or fixed partial dentures.

Patients were excluded on the basis of presence of relevant medical conditions contraindicating surgical interventions, tobacco smoking, presence of periodontitis, full-mouth plaque score (FMPS) ≥25%, full-mouth bleeding score (FMBS) ≥25%, erratic compliance with a regular supportive periodontal therapy (SPT) program.

Clinical procedures: All implants included in the study had been placed following the classic, two-stage protocol according to the manufacturer's instruction. One hour prior to surgery, the patients received 1 g amoxicillin and were prescribed 1 g twice a day for a week after the surgical procedure. Surgery was performed under local anesthesia (octocaine 20 mg/ml, with adrenaline, 1:80,000). Patients were prescribed an analgesic (Ibuprofene, DOC Generici S.r.l., Milano, Italy, 600 mg) immediately after the surgical intervention and after 8 h, and a chlorhexidine–digluconate solution 0.12% rinse (twice daily for one minute). Sutures were left in place for 10 days. The second-stage surgery and the installation of the healing cap were performed 3–6

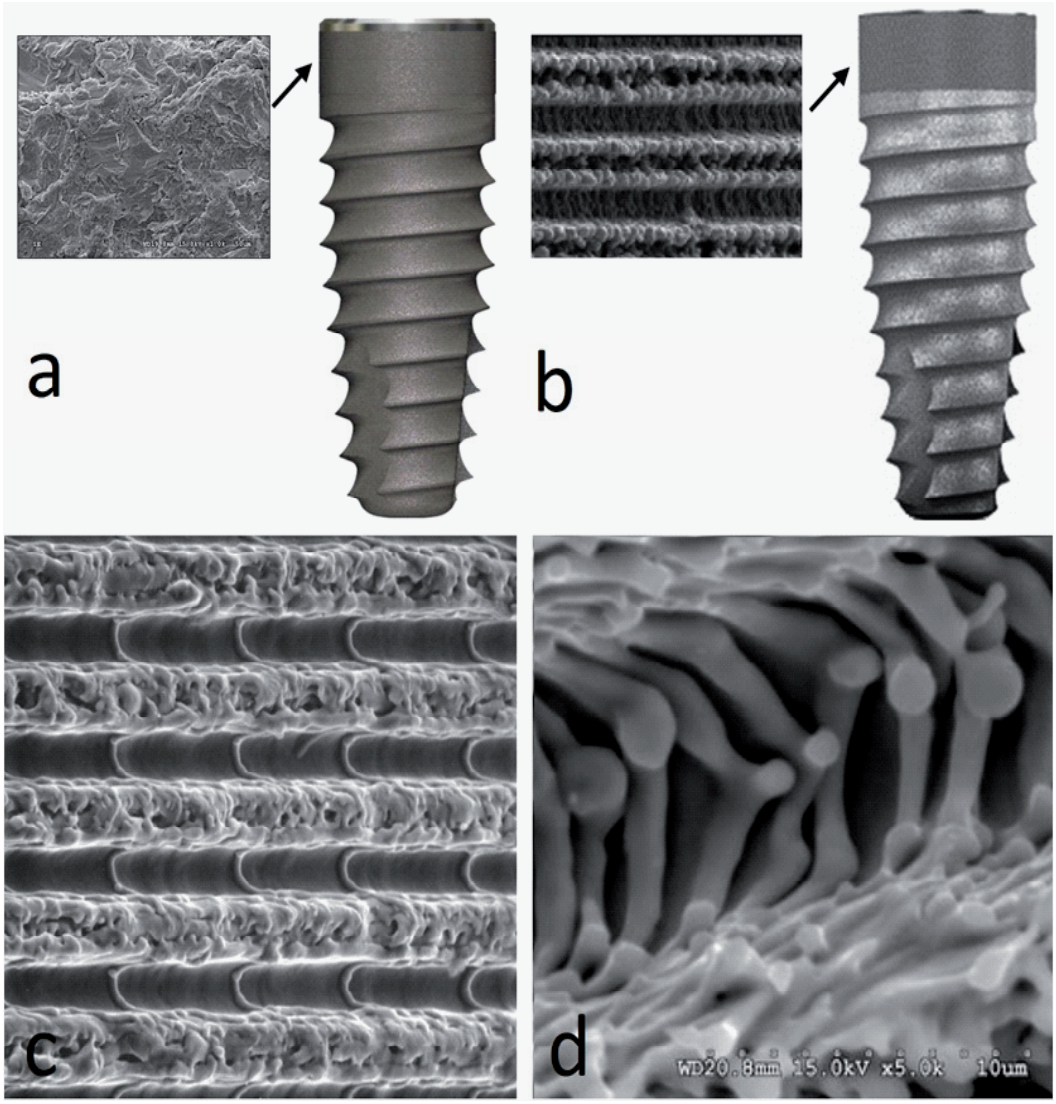

Fig. 1. Implant without LAM collar surface (a) and implant with LAM collar surface (b). Laser-ablated micron-scale modification (LAM) of the implant collar surface at SEM, magnification x800 (c) and x5000 (d), (image courtesy of BioHorizons).

months thereafter. Definitive crowns were cemented 4–6 months after second-stage surgery.

Radiographic analysis

Radiographic examinations were performed at time of crowns placement (baseline BSL), and after 3 and 5 years of observation. All the radiographs were taken by applying the long cone technique and using a film holder. A silicone index material was fixated to the residual dentition and a radiograph holder was constructed for each patient. This technique ensured that the same position of the radiograph film could be reproduced at each visit and the angle of the radiograph would not deviate.

The radiographs were taken in high resolution mode (Vista Scan Durr Dental, Durr Dental Italy S.r.l) with a dental x-ray machine (TM 2002 Planmeca Proline CC, Planmeca Group Helsinki, Finland) equipped with a long tube that operated at 70 Kw/7.5 mA., total aluminum filtration of 3.22 mm, and focus distance of 40 cm. The exposure times were 0.65 seconds for maxilla and 0.55 seconds for mandible. Specialized software (DBSWIN software, Durr Dental Italy S.r.l) was used for linear measurements of vertical peri-implant marginal bone level (VPMBL). The following radiographic measurements were performed: radiographic implant length (IL) : distance (in mm) between the implant coronal margin and the implant apex as assessed at the mid portion of the implant; residual bone height at the mesial and distal aspects of the implant: distance (in mm) between the line linking the coronal implant margin, and the first contact of the crestal bone on both mesial and distal side of the implant. To account for radiographic distortion, radiographic measurements on each radiograph were adjusted for a coefficient derived from the ratio: true length of the implant/IL. Taking as reference the collar of the implant, radiographic MBL was assessed at the mesial and the distal sides by subtracting marginal bone level at baseline from marginal bone levels at 3- (T3) and 5-year follow-up (T5).

Selection of regions of interest and fractal analysis: According to method described by Mu et al. (28), the region of interest (ROI) was set to a width of 100 pixels and height of 200 pixels (1.0 mm × 2.0 mm) close to the border of the implant at the mesial and distal aspects. The ROIs avoided crestal bone, neighboring tooth roots and lamina dura, the sinus floor, and other structural entities. The ROI was blurred using a Gaussian filter (sigma, 35 pixels; kernel size, 33 × 33). The heavily blurred image was then subtracted from the original, and 128 was added to the result at each pixel location. This generated an image with a mean grayscale value of 128, regardless of its initial intensity. The image was then made binary with a threshold brightness value of 128, and eroded and dilated once to reduce noise. The image of the trabeculae was then inverted and skeletonized. Fractal analysis was performed using the box-counting method. Using imaging software (Image J 1.43u; Wayne Rasband, National Institutes of Health, Bethesda, MD, USA), calibration was performed using the known distance of the spherical metal bearing (5.5 mm). Fractal dimensions were compared by using radiographs taken immediately after prosthesis delivery and those taken 3 and 5 years after functional loading (Fig. 2). Intra-observer agreement on ROI placement was assessed by re-evaluation of all of the images twice, with a 3-week interval between viewings.

Statistical analysis

The Wilcoxon signed-rank test was used to analyze differences in the fractal dimension before and 3 and 5 years after crowns delivery between the groups. Non-parametric methods (Kruskal–Wallis test) were used to compare MBL within and between groups, at BSL and at 3 and 5 years follow-up. Computer software MedCalc ver. 11.2.1.0 (MedCalc, Ostend, Belgium) was used to process the data. The values were deemed statistically significant when $P<0.05$. The intraobserver agreement reliability was evaluated by calculating Cronbach alpha coefficients.

Results

Forty-five patients (21 patients in the TG; mean age 47.2 ± 10.7 years and 24 patients in the CG; mean age 47.7 ± 12 years) were available for the analysis (Table 1). Table 2 and the figures 3 and 4 show differences in MBL and fractal dimensions recorded during the study period. At the end of the 5-year follow-up, the MBL in the TG was 0.87 ± 0.21 and 0.75 ± 0.25 mm at the mesial and distal aspects, respectively, while a MBL of 2.05 ± 0.25 mm at the mesial aspect and 2.01 ± 0.34 mm at the distal site was recorded in the CG. Between the two groups a statistically

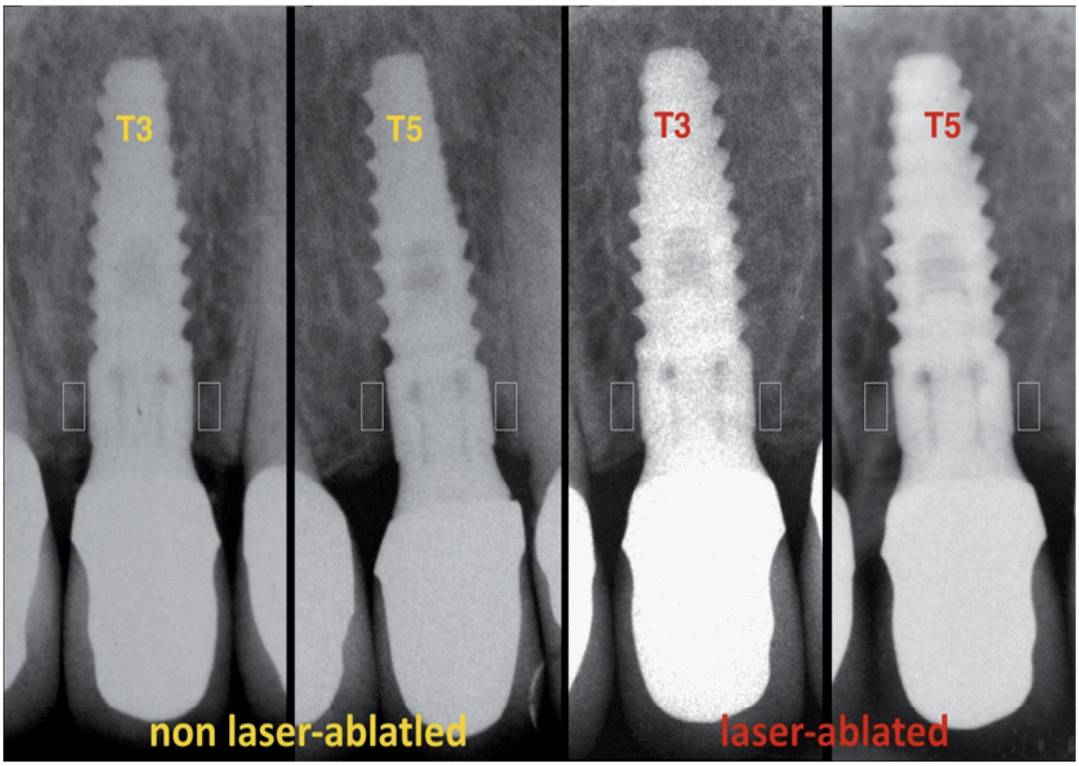

Fig. 2. Regions of interest were selected on radiographs taken immediately after prosthesis delivery, after 3 years after loading (T3) and 5 years of loading (T5).

Table 1. Demographic data

Implants n. 66	**Patients n. 45**		**Position**			
	Male n. 23	Female n. 22	Mandible n. 32 Anterior	Posterior	Maxilla n. 34 Posterior	Anterior
35 TG Length 9/10.5 mm Diameter3.8/4.6mm	17 10/7 9/8	18 11/7 10/8	6 3/3 6/0	10 7/3 5/5	6 3/3 3/3	13 8/5 5/9
31 CG Length 9/10.5 mm Diameter 3.8/4.6mm	15 9/6 11/4	16 8/8 10/6	7 3/2 3/2	9 6/3 7/2	6 4/4 5/3	9 4/5 6/3

TG= Test group, CG= control group

Table 2. Mean values and (SD) of MBL and fractal dimensions recorded during the study period

	Baseline	**3-year**	**5-year**
Mean MBL (mm) TG CG	 0.32 (0.43) 0.29 (0.36)	 0.65 (0.36) 1.74 (1.27) p = 0.0348*	 0.81 (0.21) 2.32 (1.82)
Fractal Dimensions TG CG	p = 0.0129** 1.4213 (0.0525) 1.4119 (0.0414) p = 0.0285**	1.4329 (0.0479) 1.4282 (0.0324)	1.4327 (0.0291) 1.4111 (0.0624) p = 0.0314**

TG= Test group, CG= control group
. Kruskal–Wallis test
.. Wilcoxon signed-rank test

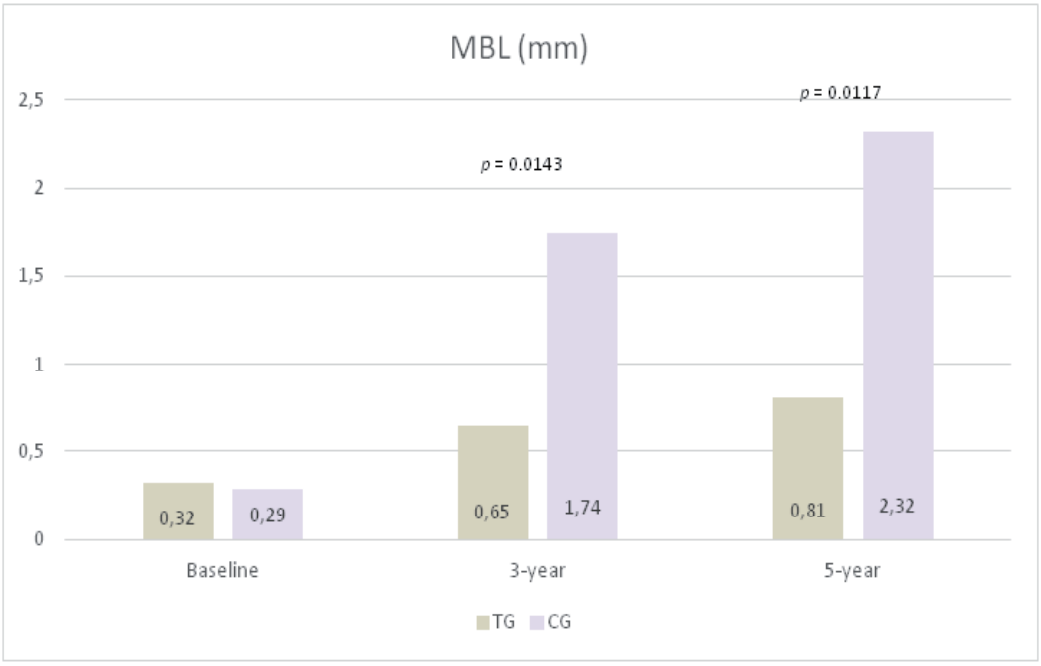

Fig. 3. Mean values of MBL recorded around test group (TG) and control group (CG) during the study period (p = Kruskal–Wallis test)

Table 3. Mean values of MBL and fractal dimensions recorded during the study period according to examinated variables.

	Baseline		3-year		5-year	
Mean MBL (mm)	**TG**	**CG**	**TG**	**CG**	**TG**	**CG**
Male/female	**0.31/0.29**	**0.29/0.32**	**0.63/0.67**	**1.76/1.72**	**0.80/0.83**	**2.30/2.34**
Mandible/maxilla	**0.28/0.32**	**0.31/0.30**	**0.61/0.68**	**1.73/1.76**	**0.81/0.82**	**2.28/2.37**
Anterior/posterior	**0.30/0.31**	**0.33/0.29**	**0.65/0.65**	**1.72/1.78**	**0.78/0.86**	**2.31/2.33**
Implant length 9/10.5 mm	**0.32/0.30**	**0.29/03.1**	**0.62/0.66**	**1.71/1.79**	**0.78/0.85**	**2.30/2.33**
Implant diameter 3.8/4.6 mm	**0.31/0.31**	**0.31/0.32**	**0.60/0.67**	**1.76/1.74**	**0.80/0.81**	**2.32/2.26**
Fractal dimensions						
Male/female	**1.4213/1.4218**	**1.4119/1.4220**	**1.4327/1.4329**	**1.4282/1.4280**	**1.4325/1.4329**	**1.4111/1.4110**
Mandible/maxilla	**1.4220/1.4214**	**1.4123/1.4216**	**1.4330/1.4325**	**1.4284/1.4278**	**1.4324/1.4330**	**1.4109/1.4112**
Anterior/posterior	**1.4218/1.4222**	**1.4120/1.4224**	**1.4331/1.4328**	**1.4280/1.4282**	**1.4327/1.4328**	**1.4113/1.4108**
Implant length 9/10.5 mm	**1.4216/1.4220**	**1.4115/1.4223**	**1.4324/1.4333**	**1.4281/1.4279**	**1.4328/1.4326**	**1.4112/1.4109**
Implant diameter 3.8/4.6 mm	**1.4218/1.4216**	**1.4120/1.4219**	**1.4326/1.4330**	**1.4286/1.4276**	**1.4326/1.4327**	**1.4113/1.4107**

TG= Test group, CG= control group

significant difference was noted. In the TG the mean fractal dimension before loading was 1.4213 ± 0.0525. It increased significantly to 1.4329 ± 0.0479 at 3 years after loading and remained almost stable at 5 years after loading (1.4327 ± 0.0291). In the CG the mean fractal dimension before loading was 1.4119 ± 0.0414. It increased significantly to 1.428 ± 0.0324 at 3 years after loading and decreased significantly to 1.4111 ± 0.0624 at 5 years after loading. At the end of the follow-up, differences between both study groups were statistically significant.

In both groups, no statistical correlation was found between MBL and fractal dimension and gender, location (mandible/maxilla, anterior/posterior), implant lenght and diameter (Table 3).

Discussion

Although in orthopedics the paradigm of "bone quality" has already shifted from bone mineral densities (BMD) -based assessments to microstructural evaluations of bone (bone architecture, bone turnover, bone mineralization, and micro-damage accumulation), BMDs-based diagnosis on radiographic evaluations, still remains challenging in implant dentistry because devices capable of accurately evaluating bone structure have yet to be developed. (29) One quantitative method to analyze the bone density in periapical radiographs is represented by fractal dimension analysis. Fractal analysis is based on fractal mathematics for describing complex shapes and structural patterns (24). It indicates a figure's complexity and is expressed numerically as "fractal dimension", which measures self-similarity. Trabecular bone has a branching pattern that exhibits fractal properties, such as self-similarity and lack of well-defined scale. Therefore, when applied to trabecular bone images on radiographs, this method can be considered as a reflection of trabecular bone microarchitecture. In addition, it is reported that fractal analysis is not affected by variations in exposure, alignment and choice of ROI, which may be another advantage of this method in clinical settings (30,31). In the present study after 3 years of loading, both groups of implants showed an increase of the fractal dimension ($P < 0.05$) without differences between the groups, suggesting an increase in the amount of peri-implant bony microstructure. This results is in agreement with data reported by other studies which found an increased fractal dimension after implant loading (32,33). Implants exposed to functional loading exhibit signs of bone remodeling, including the presence of bone multicellular units and a higher degree of bone-implant contact (34-36). Mechanical loading also increases the bone volume fraction and trabecular thickness and content, and alters trabecular morphology (37). Unlike the one registered after 3 years of loading, at 5 years of loading, compared to TG, the CG showed a statistically significant decrease of the fractal dimension. In addition, at the end of the follow-up period, the CG showed also a statistically significant increase of MBL. A possible explanation of this results could be linked with the ability of the LAM of collar surface to create a soft tissue seal that protects the underline bone from the oral environment. The presence of granulation tissue in contact with the transmucosal titanium surfaces is thought to be one of factors favoring apical epithelial migration, and the related MBL (38). Material properties appear to be another factor affecting epithelial downgrowth. Kim et al. (39) compared the effects of abutment shapes relative with MBL. They compared implants with laser micro-textured transmucosal profiles, machined profiles, and straight anodically oxidized profiles. Around machined and anodically oxidized profiles, the junctional epithelium was found longer, around laser-microtextured profiles epithelium was shorter, connective tissue attachment was more extended and the bone-level stable. Furthermore, a recent gene profiling analysis (40) documented that the mucosal wound healing around dental implants is influenced by the topographic nature of the coronal surface. In biopsies obtained after 2, 4, and 8 weeks, at the laser-microtextured vs. machined implant collar surface, a differential gene expression was revealed. mRNAs encoding keratins and protective proteins of cornified epithelium were upregulated in tissues from laser-modified surfaces. Moreover, in tissue from laser-modified surfaces,

upregulation of mRNAs encoding proteins associated with collagen fibril formation and function was observed at 4 weeks. Based on these data, one might speculate that repetitive nanosize surface features created with a laser on the implant collar have the ability to influence the soft tissue healing around dental implants. As in the case around natural teeth, in which collagen bundles inserted into the root cementum deter the downgrowth migration of the overlying epithelium, epithelial downgrowth around implants could be impeded by firm physical attachment between the soft connective tissue and the implant (41-45). The laser-microtextured surface, although not analogous to the cemental surface of the natural teeth, seems to act in establishing a predetermined site to attract a physical connective tissue attachment, to restrict apical migration of gingival epithelium, and thus to preserve the coronal level of bone.

Conclusions: The increased fractal dimension and the reduced MBL around TG implants after 5 years of functional loading indicates an positive effect of a laser-ablated micron-scale modication of collar surface on peri-implant trabecular bone remodeling.

Acknowledgments

The authors declare that they have not any financial affiliations or conflicts of interests.

References

1. Guarnieri R, Placella R, Testarelli L, et al. Clinical, radiographic, and esthetic evaluation of immediately loaded laser microtextured implants placed into fresh extraction sockets in the anterior maxilla: a 2-year retrospective multicentric study. Implant Dent. 2014; 23:144-54
2. Passariello C, Di Nardo D, Testarelli L. Inflammatory perimplant diseases and the periodontal connection question. Eur J Dent. 2019; 13:119-123
3. Albrektsson T, Zarb G, Worthington P, et al. The long term efficacy of currently used dental implants: a review and proposed criteria of success. Int J Oral Maxillofac Impl. 1986; 1:11–25
4. Albrektsson T, Donos N, Working Group 1. Implant survival and complications. The Third EAO consensus conference. Clin Oral Impl Res. 2012; 23:63–65
5. Hermann JS, Cochran DL, Nummikoski PV, et al. Crestal bone changes around titanium implants. A radiographic evaluation of unloaded non submerged and submerged implants in the canine mandible. J Periodontol. 1997;68:1117–1130
6. Sanz M, Klinge B, Alcoforado G, et al. Biological aspects: Summary and consensus statements of group 2. The 5th EAO Consensus Conference 2018. Clin Oral Implants Res. 2018; 29:157-159
7. Bateli M, Att W, Strub JR. Implant neck configurations for preservation of marginal bone level: a systematic review. Int J Oral Maxillofac Impl. 2011; 26:290–303
8. Tomasi C, Tessarolo F, Caola I, et al. Early healing of peri-implant mucosa in man. J Clin Periodontol. 2016; 43:816–824
9. Wang RC, Hsieh MC, Lee TM. Effects of nanometric roughness on surface properties and broblast's initial cytocompatibilities of Ti6Al4V. Biointerphases. 2011; 6:87
10. Ricci JL, Grew JC, Alexander H. Connective-tissue responses to defined biomaterial surfaces. I. Growth of rat fibroblast and bone marrow cell colonies on microgrooved substrates. J Biomed Mater Res A. 2008; 85:313–325
11. Ricci JL, Grew JC, Alexander H. Connective-tissue responses to defined biomaterial surfaces. II. Behavior of rat and mouse fibroblasts cultured on microgrooved substrates. J Biomed Mater Res A. 2008; 85:326–335
12. Dumas V, Rattner A, Vico L, et al. Multiscale grooved titanium processed with femtosecond laser influences mesenchymal stem cell morphology, adhesion, and matrix organization. J Biomed Mater Res A. 2012; 100:3108–3116
13. Nevins M, Kim DM, Jun SH, et al. Histologic evidence of a connective tissue attachment to laser microgrooved abutments: A canine study. Int J Periodontics Restorative Dent. 2010; 30:245–255
14. Shin SY, Han DH. Influence of microgrooved collar design on soft and hard tissue healing of immediate implantation in fresh extraction sites in dogs. Clin Oral Impl Res. 2010;21:804–814.
15. Nevins M, Nevins ML, Camelo M, et al. Human histologic evidence of a connective tissue attachment to a dental implant. Int J Periodontics Restorative Dent. 2008; 28:111–121
16. Lollobrigida M, Fortunato L, Serafini G, et al. The Prevention of Implant Surface Alterations in the Treatment of Peri-Implantitis: Comparison of Three Different Mechanical and Physical Treatments. Int J Environ Res Public Health. 2020; 17:2624
17. Guarnieri R, Di Nardo D, Di Giorgio G, et al. Influence of the Microgap/Interface Vertical Position on Early Marginal Bone Remodeling Around One-Stage Implants with Laser-Microtextured Collar Surface: A Randomized Clinical Study. Int J Periodontics Restorative Dent. 2019; 39:553-60
18. Guarnieri R, Di Nardo D, Gaimari G, et al. Influence of restorative margins position on one-stage laser-microgrooved implants-supported single screwed crowns: A clinical, biochemical, and microbiological analysis. Clin Implant Dent Relat Res. 2019; 21:52-9
19. Guarnieri R, Di Nardo D, Gaimari G, et al. One-stage laser-microtextured implants immediately placed in the interradicular septum of molar fresh extraction sockets associated with GBR technique. A case series study. J Clin Exp Dent. 2018; 10:e996-e1002
20. Guarnieri R, Di Nardo D, Gaimari G, et al. Short vs. Standard Laser-Microgrooved Implants Supporting Single and Splinted Crowns: A Prospective Study with 3 Years Follow-Up. J Prosthodont. 2019; 28:e771-e779
21. Akesson L, Hakansson J, Rohlin M. Comparison of panoramic and intraoral radiography and pocket probing for the measurement of the marginal bone level. J Clin Periodontol. 1992; 19:326-32
22. Lang NP, Hill RW. Radiographs in periodontics. J Clin Periodontol. 1977; 4:16-28
23. Buckland-Wright JC, Lynch JA, Rymer J, et al. Fractal signature analysis of macroradiographs measures trabecular organization in lumbar vertebrae of postmenopausal women. Calcif Tissue Int. 1994; 54:106-12
24. Fazzalari NL, Parkinson IH. Fractal properties of cancellous bone of the iliac crest in vertebral crush fracture. Bone. 1998;23:53-7

25. Caligiuri P, Giger ML, Favus M. Multifractal radiographic analysis of osteoporosis. Med Phys 1994;21:503-8
26. Wilding RJ, Slabbert JC, Kathree H, et al. The use of fractal analysis to reveal remodelling in human alveolar bone following the placement of dental implants. Arch Oral Biol. 1995; 40:61-72
27. Southard TE, Southard KA, Jakobsen JR, et al. Fractal dimension in radiographic analysis of alveolar process bone. Oral Surg Oral Med Oral Pathol Oral Radiol Endod. 1996; 82:569-76
28. Mu TJ, Lee DW, Park KH, et al. Changes in the fractal dimension of peri-implant trabecular bone after loading: a retrospective study. J Periodontal Implant Sci. 2013; 43(5):209-14
29. Southard TE, Southard KA. Detection of simulated osteoporosis in maxillae using radiographic texture analysis. IEEE Trans Biomed Eng. 1996; 43:123-32
30. Jolley L, Majumdar S, Kapila S. Technical factors in fractal analysis of periapical radiographs. Dentomaxillofac Radiol. 2006; 35:393–397
31. Shrout MK, Potter BJ, Hildebolt CF. The effect of image variations on fractal dimension calculations. Oral Surg Oral Med Oral Pathol Oral Radiol Endod. 1997; 84:96–100
32. Mu TJ, Lee DW, Park KH, et al. Changes in the fractal dimension of peri-implant trabecular bone after loading: a retrospective study. J Periodontal Implant Sci. 2013; 43:209-14
33. Wilding RJ, Slabbert JC, Kathree H, et al. The use of fractal analysis to reveal remodelling in human alveolar bone following the placement of dental implants. Arch Oral Biol. 1995; 40:61-72
34. Ogiso M, Tabata T, Kuo PT, et al. A histologic comparison of the functional loading capacity of an occluded dense apatite implant and the natural dentition. J Prosthet Dent. 1994; 71:581-8
35. Piattelli A, Corigliano M, Scarano A, et al. Immediate loading of titanium plasma-sprayed implants: an histologic analysis in monkeys. J Periodontol. 1998; 69:321-7
36. Gotfredsen K, Berglundh T, Lindhe J. Bone reactions adjacent to titanium implants subjected to static load. A study in the dog (I). Clin Oral Implants Res. 2001; 12:1-8
37. Roberts WE, Smith RK, Zilberman Y, et al. Osseous adaptation to continuous loading of rigid endosseous implants. Am J Orthod. 1984; 86:95-111
38. Listgarten MA. Soft and hard tissue response to endosseous dental implants. Anat Rec 1996; 245:410-25
39. Kim S, Oh KC, Han DH, et al. Influence of transmucosal designs of three one-piece implant systems on early tissue responses: a histometric study in beagle dogs. Int J Oral Maxillofac Implants. 2010; 25:309-14
40. Leong A, De Kok I, Mendonça D, et al. Molecular_Assessment_of Human Peri-implant Mucosal Healing at Laser-Modified and Machined Titanium Abutments. Int J Oral Maxillofac Imp. 2018;33:895-904.
41. Di Carlo S, De Angelis F, Ciolfi A, et al. Timing for implant placement in patients treated with radiotherapy of head and neck. Clin Ter. 2019;170:e345-e351
42. Lorenzi C, Arcuri L, Lio F, et al. Radiosurgery in dentistry: a review. Clin Ter. 2019;170:e48-e54.
43. Pandolfi A. A modified approach to horizontal augmention of soft tissue around the implant: omega roll envelope flap. Description of surgical technique. Clin Ter. 2018;169:e165-e169
44. Brauner E, De Angelis F, Jamshir S, et al. Aesthetic satisfaction in lip and palate clefts: a comparative study between secondary and tertiary bone grafting. Clin Ter. 2018;169:e62-e66
45. Brauner E, Quarato A, De Angelis F, et al. Prosthetic rehabilitation involving the use of implants following a fibula free flap reconstruction in the treatment of Osteosarcoma of the maxilla: a case report. Clin Ter. 2017;168:e392-e396